

## ZnO metal-semiconductor field-effect transistors with Ag-Schottky gates

H. Frenzel,<sup>a)</sup> A. Lajn, M. Brandt, H. von Wenckstern, G. Biehne, H. Hochmuth, M. Lorenz, and M. Grundmann

Universität Leipzig, Fakultät für Physik und Geowissenschaften, Institut für Experimentelle Physik II, Linnéstrasse 5, 04103 Leipzig, Germany

(Received 1 April 2008; accepted 22 April 2008; published online 14 May 2008)

Metal-semiconductor field-effect transistors (MESFETs) were fabricated by reactive dc sputtering of Ag-Schottky gate contacts on ZnO thin-film channels grown by pulsed-laser deposition on sapphire. The  $n$ -type conductivity (normally on) of typical MESFETs is tunable over 8 decades in a voltage range of 2.5 V with an off voltage of  $-1.5$  V and very low off-current density in the range of  $10^{-6}$  A/cm<sup>2</sup>. Channel mobilities of up to 27 cm<sup>2</sup>/V s have been achieved. © 2008 American Institute of Physics. [DOI: 10.1063/1.2926684]

Transparent ZnO field-effect transistors have been intensively studied in the past few years to achieve possible applications in active-matrix thin-film transistor (TFT) displays. Besides transparency, their advantages are the higher channel mobility compared to the currently used poly-Si TFTs (Ref. 1) and cheaper production cost. Up to now mostly metal-insulator-semiconductor structures (MISFETs) are used for those purposes due to the simple realization of high- $k$  insulators by rf-sputtering techniques.<sup>2,3</sup> However, the key advantage of metal-semiconductor FETs (MESFETs) is the higher mobility of carriers in the channel, as compared to MISFETs. Since the carriers in the channel of a MISFET are accelerated toward the semiconductor/insulator interface by the gate electric field where they suffer interface scattering, their mobility is less than half of the mobility of bulk material. As the depletion region in MESFETs keeps the carriers off the gate interface, their mobility is close to that of bulk material. The higher mobility leads to a higher current, transconductance and transit frequency of the device.<sup>4</sup>

Up to now, the difficulties of ZnO MESFETs lie in the fabrication of high-quality Schottky contacts on ZnO. Ryu *et al.* reported on MESFETs on  $p$ -type ZnO using Ni and Ti metals as Ohmic and Schottky contacts,<sup>5</sup> respectively. Their output characteristics show that pinch off and saturation are barely obtained for large source-drain voltages in the range of 10 V before breakdown. The gate voltage had to be as large as 20 V to switch the MESFET over only 1 mA. Kandasamy *et al.* used a Pt Schottky gate/ $n$ -type ZnO MESFET for hydrogen gas sensing applications.<sup>6</sup> Their saturation current had a positive slope which does not correspond to ideal MESFET characteristics but served the purpose of sensing different hydrogen gas concentrations.

We report on the fabrication of  $n$ -type ZnO MESFETs with excellent electric properties which can be used for low signal processing in future ZnO-based optoelectronic devices. The effect of low doping and very thin channels on the output and transfer characteristics of the MESFETs is investigated.

The ZnO thin films were grown by pulsed-laser deposition on  $a$ -plane sapphire substrates at a growth temperature of about 630 °C and an oxygen partial pressure of 0.02 mbar. Four layer configurations, denoted as samples 1,

2, 3, and 4 (cmp. Table I), have been used: either 10 000 or 3000 pulses of ZnO, directly grown on the substrate and on a MgO buffer layer, respectively. The MgO buffer, which has been *in situ* annealed for 20 min at  $5 \times 10^{-5}$  mbar, drastically reduces the Al diffusion from the substrate into the ZnO layer.<sup>7</sup> The thicknesses  $d$  of the ZnO layers measured by spectroscopic ellipsometry, mobilities, and charge carrier concentrations obtained from Hall effect measurements are shown in Table I. A lower doping concentration leads to a larger depletion layer depth under the Schottky gate contact and therefore to a lower off voltage of the MESFET. In the ideal case, a “normally off” FET can be achieved, which is advantageous for low-power circuits.

Three photolithography steps were used to produce the MESFETs, as depicted in Fig. 1. First, a mesa structure was etched into the ZnO with phosphorous acid to form channels. Then the Ohmic source and drain contacts were deposited by dc sputtering of Au under 0.02 mbar Ar atmosphere. The dc-sputtered Au contacts form Ohmic contacts on  $n$ -ZnO, as reported elsewhere.<sup>8</sup> Last, highly rectifying Ag-Schottky gate contacts were fabricated using reactive dc sputtering under a 50/50 ratio of O<sub>2</sub> and Ar at 0.02 mbar. This method was adapted from Allen *et al.*<sup>9</sup> and optimized for our thin films. Subsequently, an Au-capping layer was sputtered for passivation.

$I$ - $V$  characteristics of the gate Schottky contacts are depicted in Fig. 2. They show an excellent rectification behavior with leakage currents in the range of picoamperes. For samples 2 and 3 an ideality factor of 1.6 was calculated whereas it is 2.0 for sample 1 and 3.0 for sample 4. The Schottky barrier height is 1.0 V for all samples. The forward current is limited by the series resistances  $R_S$  of the ZnO layers, which are 5 k $\Omega$  for S1 and S3, 1 M $\Omega$  for S2, and 200 M $\Omega$  for S4. Here, the effect of the MgO buffer layer on  $R_S$  is obvious. The rectification ratios, corrected for  $R_S$ , at  $\pm 2$  V are  $10^8$  for S2,  $2 \times 10^8$  for S3,  $1.5 \times 10^7$  for S1, and  $3 \times 10^5$  for S4. The excellent properties of the Ag-Schottky contacts probably result from oxygen plasma etching of the ZnO surface during the first seconds of reactive dc sputtering.

$I$ - $V$  and FET output and transfer characteristics were measured using an Agilent 4156C precision semiconductor parameter analyzer on a SÜSS Waferprober with tungsten probes. Samples 2 and 3 showed a typical field-effect behavior, whereas samples 1 and 4 represent two nonideal cases. In

<sup>a)</sup>Electronic mail: HFrenzel@physik.uni-leipzig.de. URL: <http://www.uni-leipzig.de/~hlp/>.

TABLE I. Overview of the measured sample properties.

Sample	Layers	$d$ (nm)	$n$ ( $\text{cm}^{-3}$ )	$N_D - N_A$ ( $\text{cm}^{-2}/\text{V s}$ )	$\mu_{\text{Hall}}$ $\text{cm}^{-3}$	$\mu_{\text{ch}}$ ( $\text{cm}^2/\text{V s}$ )	$g_{\text{max}}$ (S/cm)	rect. ratios ( $R_S$ corr.)
S1	10 000 pulses ZnO	131	$1.5 \times 10^{18}$	$5 \times 10^{17}$	15.4	19.1	10.2	$1.5 \times 10^7$
S2	10 000 pulses ZnO+MgO	117	$2.9 \times 10^{13}$	$1.5 \times 10^{14}$	29.4	27.4	$4.4 \times 10^{-3}$	$1 \times 10^8$
S3	3000 pulses ZnO	20	$5.5 \times 10^{17}$	$2.5 \times 10^{18}$	9.3	11.3	30.3	$2 \times 10^8$
S4	3000 pulses ZnO+MgO	32	$4.7 \times 10^{12}$	...	9.7	...	...	$5 \times 10^5$

case of sample 1, the high doping concentration leads to a smaller depletion layer width. A large reverse Schottky-gate voltage needs to be applied to show any field effect on the source drain current. However, the gate leakage current limits the applicable gate voltage. The comparatively thick channel cannot be completely depleted. So, pinch off and saturation could not be observed. On the other hand, the low doping concentration and thinner channel of sample 4 leads to a fully depleted channel for all applied gate voltages. This FET cannot be switched on.

The output characteristics of sample 3 are shown in Fig. 3(a). The pinch-off points follow a quadratic behavior as predicted by MESFET theory.<sup>10</sup> At these points, the depletion layer of the Schottky contact is deformed by the source-drain voltage such that it completely closes the channel and only a constant diffusive saturation current flows. Sample 2 showed an equivalent FET behavior (not shown here). However, a lower source-drain current due to the lower doping concentration has been observed. Furthermore, the larger gate leakage current has a detrimental effect on the FET performance.

A comparison of transfer characteristics for samples 1, 2, and 3 at source-drain voltage  $V_{\text{SD}}=4$  V is shown in Fig. 3(b). As mentioned above, sample 1 is not in the saturation regime at  $V_{\text{SD}}=4$  V. Nevertheless, the curve is shown for comparison. Samples 2 and 3 show a strong field effect. The channel current of sample 3 can be tuned over 8 orders of magnitude in a gate-voltage range of only 2.5 V. Both MESFETs exhibit “normally on” behavior having the same off voltage of  $-1.5$  V. The off current is limited by the Schottky contact’s leakage current whereas the on current reflects the channel’s series resistance. It can also be seen that the slope of  $I_{\text{SD}}$  versus  $V_G$  for sample 3 is higher than for sample 2 which reflects the higher maximum forward saturation transconductance being equal to the maximum drain transconductance

$g_{\text{max}}$  shown in Table I. The forward gate voltage does not exceed 1 V, which is the approximate built-in voltage of the Schottky contact. Then, the depletion layer is reduced to zero and the channel is completely open. A further increase in the gate voltage does not lead to an increase in  $I_{\text{SD}}$  but to an exponential increase of gate leakage current.

In order to calculate the channel mobility  $\mu_{\text{ch}}$ , the drain transconductance  $g_D \equiv \partial I_{\text{SD}} / \partial V_{\text{SD}}$  is obtained for  $V_{\text{SD}} \rightarrow 0$  from the output characteristics. It is equal to the forward transconductance in the saturation regime  $g_{m,\text{sat}} \equiv \partial I_{\text{SD}} / \partial V_G$  and is given by<sup>10</sup>

$$g_{D0} = g_{\text{max}} \left[ 1 - \left( \frac{V_{\text{bi}} + V_G}{V_P} \right)^{1/2} \right] = g_{m,\text{sat}}, \quad (1)$$

where  $V_{\text{bi}}$  is the Schottky-contact’s built-in voltage,  $V_G$  is the gate voltage, and  $V_P$  is the pinch-off voltage of the MESFET. The maximum transconductance  $g_{\text{max}}$  can be extracted from Eq. (1) and is presented in Table I. The channel mobility is then given by

$$\mu_{\text{ch}} = \frac{g_{\text{max}}}{W/L e N_D d}, \quad (2)$$

where  $W/L=400 \mu\text{m}/60 \mu\text{m}$  is the channel’s width to length ratio,  $e$  is the elementary charge, and  $d$  is the channel depth. The doping concentration  $N_D - N_A$  is obtained from capacitance-voltage ( $C-V$ ) measurements using an Agilent 4294A precision impedance analyzer. For samples 2 and 3, it could be determined without difficulty from the  $1/C^2$  behavior. In case of sample 4, there was no capacitance measurable within the precision of femtofarads. The  $C-V$  measurements of sample 1 indicated the presence of a degenerated layer at the ZnO-channel/substrate interface due to accumulation of Al. In this case, it was not possible to directly determine  $N_D - N_A$  due to the rapidly increasing conductance for positive gate voltages. It was instead determined by comparison

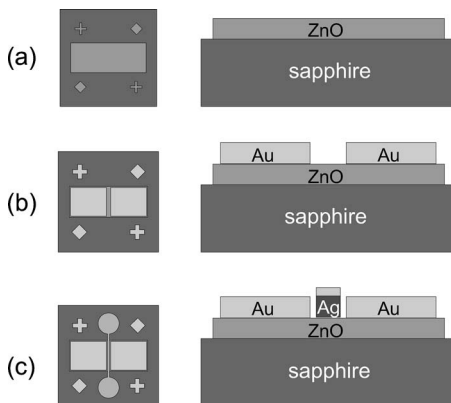


FIG. 1. Top view and side view of the MESFET photolithography steps: Mesa etching (a), deposition of source/drain contacts (b), and gate contact (c).

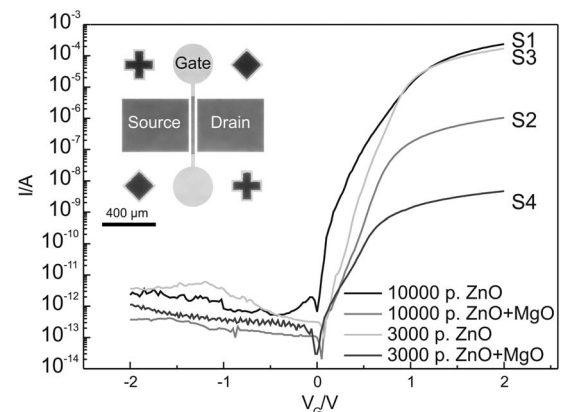


FIG. 2.  $I$ - $V$  characteristics of MESFET’s Ag-Schottky gate contacts. Inset: photograph of a MEFET.

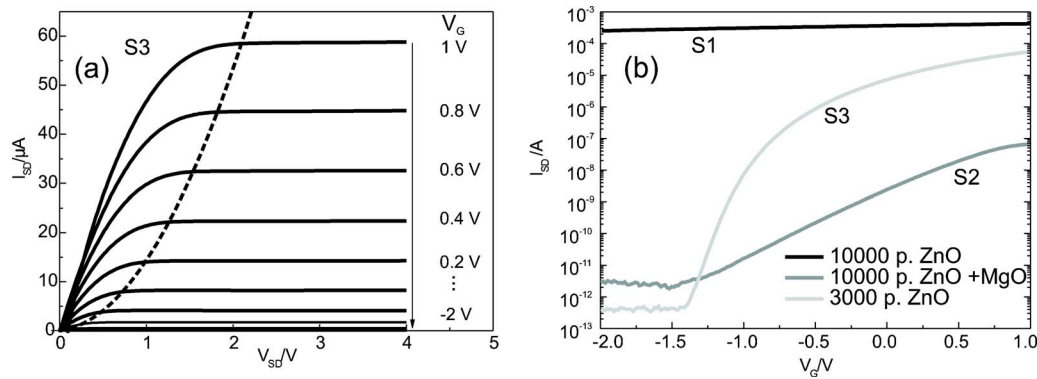


FIG. 3. (Color online) (a) Source-drain  $I$ - $V$  output characteristic of sample 3 for different gate voltages. The dashed line is a quadratic fit of the pinch-off points. (b) Transfer characteristics of samples 1, 2, and 3. (Note that sample 1 is not in saturation regime.)

of the capacitance with a MESFET sample which was grown under equal conditions where extraction of  $N_D - N_A$  was possible.

In Table I the net doping concentrations  $N_D - N_A$  calculated from  $C$ - $V$  measurements performed on the final MESFET structures are compared to free carrier densities  $n$  obtained at 300 K from Hall effect measurements on the as-grown layers. One can see that  $N_D - N_A$  of samples 2 and 3 are ten times higher than  $n$  implying that not all of the dominant donors are ionized at room temperature. Only for sample 1  $n$  equals  $N_D - N_A$  since S1 is in the saturation regime at room temperature. Hence, the thermal activation energy of the dominant donors in S1 has to be smaller than in S2 and S3.

The channel mobilities obtained from Eq. (2) are in good agreement with the Hall mobilities of the unstructured ZnO layers. This confirms that the MESFET channel mobility equals the bulk mobility of the respective semiconductor. The mobilities of samples 1 and 3 are lower than that of sample 2 due to the higher doping concentration and associated scattering at ionized impurities. However, the mobility of sample 2 is lower than typically observed mobilities for ZnO,<sup>8</sup> which may be due to the larger influence of grain boundaries.<sup>11</sup>

In summary, we have fabricated high-quality ZnO MESFETs using highly rectifying Ag Schottky contacts as gate. The MESFET's electrical behavior follows the established MESFET theory. It has been shown that the channel mobility equals the bulk mobility. Furthermore, the influence of channel thickness and doping concentration on the device performance has been demonstrated.

The authors thank Helena Hilmer and Chris Sturm for the spectroscopic ellipsometry measurements and gratefully acknowledge financial support of this work by Deutsche Forschungsgemeinschaft in the framework of Sonderforschungsbereich 762 "Functionality of Oxidic Interfaces" and the Graduate School "Leipzig School of Natural Sciences-Build-MoNa."

<sup>1</sup>J. F. Wagner, *Science* **300**, 1245 (2003).

<sup>2</sup>J. Nishii, A. Ohtomo, K. Ohtani, H. Ohno, and M. Kawasaki, *Jpn. J. Appl. Phys., Part 2* **40**, L1193 (2005).

<sup>3</sup>K. Ueno, I. H. Inoue, H. Akoh, M. Kawasaki, Y. Tokura, and H. Takagi, *Appl. Phys. Lett.* **83**, 1755 (2003).

<sup>4</sup>B. V. Zeghbroeck, *Principles of semiconductor devices*, URL <http://ece-www.colorado.edu/~bart/book/book/index.html>.

<sup>5</sup>Y. R. Ryu, T. S. Lee, J. A. Lubguban, H. W. White, Y. S. Park, and C. J. Youn, *Appl. Phys. Lett.* **87**, 153504 (2005).

<sup>6</sup>S. Kandasamy, W. Wlodarski, A. Holland, S. Nakagomi, and Y. Kokubun, *Appl. Phys. Lett.* **90**, 064103 (2007).

<sup>7</sup>H. von Wenckstern, S. Weinhold, G. Biehne, R. Pickenhain, H. Schmidt, H. Hochmuth, and M. Grundmann, *Adv. Solid State Phys.* **45**, 263 (2005).

<sup>8</sup>H. von Wenckstern, M. Brandt, J. Lenzner, G. Zimmermann, H. Hochmuth, M. Lorenz, and M. Grundmann, *Zinc Oxide and Related Materials*, edited by J. Christen, C. Jagadish, D. C. Look, T. Yao, and F. Bertram, CMRS Symposia No. 957 (Materials Research Society, Pittsburgh, 2007), 0957-K03-02.

<sup>9</sup>M. W. Allen, S. M. Durbin, and J. B. Metson, *Appl. Phys. Lett.* **91**, 053512 (2007).

<sup>10</sup>M. Grundmann, *The Physics of Semiconductors-An Introduction Including Devices and Nanophysics* (Springer, Berlin, Heidelberg, New York, 2006).

<sup>11</sup>J. W. Orton, B. J. Goldsmith, M. J. Powell, and J. A. Chapman, *Appl. Phys. Lett.* **37**, 557 (1980).